Iranian Journal of Mechanical Engineering
The Iranian Society of Mechanical Engineers
Research Paper

DOI: 10.30506/JMEE.2021.141838.1244

Study of Flow over Bluff Bodies using Combination of FD-CVC Methods

M. Mohseni[*]
Ph.D. Student

S. M. Malek Jafarian[†]
Associated Professor

FD-CVC (Feature Detection-Compressible Vorticity Confinement) methods were introduced by the authors in the past [1] and its result for some simple problems was investigated. In the present study, FD-CVC methods are used to study vortex flows around bluff bodies such as projectile and square cylinder. The ability and flexibility of the methods in more complex and applied problems are studied in this paper. It is observed that using the FD-CVC methods, by limiting the effect of vorticity confinement to the points needed, improve the results. It is seen the proper functioning of these methods on various confinement parameters (using threshold function) shows the superiority of the present method over the standard CVC method.

Keywords: Threshold Function, Confinement Parameter, Vortex Flows, Feature Detection Method, Compressible Vorticity Confinement.

1 Introduction

Problems like the flow around large buildings, over helicopters, etc. are generally known as vortex dominant flows. The numerical solutions to these problems are coming with serious challenges. The vortices diffused and dissipated at a higher rate than the reality, due to the errors caused by the discretization of the equations. To overcome this problem, different methods have been considered, such as using a finer grid, adaptive grid generation, and high order discretization schemes. On the other hand, these methods increase computational time and complication of the numerical codes. Furthermore, the vorticity confinement method introduces a simple and low cost solution to solve this difficulty; this has resulted in an attractive topic for this research.

Steinhoff and Steinhoff et al. presented the vorticity confinement methods for incompressible flows in their research [2, 3] for the first time. In the Steinhoff proposed method, the artificial viscosity error was improved by adding a source term to the momentum equation. Many researchers tried to develop this method for compressible flows. Hu et al. proposed a compressible vorticity confinement method that did not have the problems of previous methods [4]. Hereafter, several types of research have been carried out in this field. Some of the recent studies are: The ability and efficiency of a compressible vorticity confinement in a high-order flow solver for prediction of compressible mixing layer flows on coarse grids was investigated

[*]Ph.D. student, Department of Mechanic Engineering, University of Birjand, Birjand, South Khorasan, 97175/615, Iran, Mostafa65.mohseni@gmail.com

† Corresponding Author, Associate Professor, Department of Mechanical Engineering, University of Birjand, Birjand, South Khorasan, 97175/615, Iran, mmjafarian@birjand.ac.ir
Receive: 2020/12/01 Accepted: 2021/12/20

by Sadri et al. [5]. The vorticity confinement method was used by O`regan et al. for simulation of the airplane wingtip vortices [6]. A third-order vorticity confinement accuracy method was proposed by Costes et al. [7]. Petropoulos et al. increased the accuracy of the Costes et al.'s method to fifth-order [8]. Sidilkover proposed a unified numerical method that achieves both vorticity confinement and shock-capturing capabilities for compressible flow calculation. This approach can improve the resolution of vortices [9]. Sadri et al. studied numerically the fluid flow and acoustic field of a supersonic jet using high-order discretization and the vorticity confinement (VC) method on coarse grids [10]. Wen and Ma applied vorticity confinement in a vorticity preserving lattice Boltzmann method (VPLBM) to simulate the high-resolution motion of smoke in real time. The method can preserve the detailed motion of smoke [11].

Despite the suitability of the vorticity confinement method, it has a major disadvantage. The confinement parameter must be tuned by the user. Many efforts have been made to overcome this problem. Costes and Kowani used the local vorticity value to calculate the confinement parameter [12]. Robinson proposed a formulation that used helicity to define the value of the confinement parameter [13]. Malek Jafarian and Pasandideh Fard suggested three expressions for the calculation of confinement parameters that used the concept of artificial viscosity [14]. Butsuntorn and Jameson proposed a relation for the confinement parameter that depends on the cell volume and helicity value [15]. Hahn and Iaccarino introduced a formulation for the confinement parameter at incompressible flows that uses the difference in the results of upwind and central difference schemes [16]. Bagheri-Esfeh and Malek Jafarian, expanded the Hahn and Iaccarino scheme to the compressible flows [17]. Mohseni and Malek Jafarian proposed the idea of reduction of the sensitivity of the vorticity confinement method to confinement parameter variations by combining this method with the FCT scheme for various limiters. They showed that the best results were obtained using the minmod limiter at the middle step [18]. Povitsky and Pierson applied the vorticity confinement method for accurate prediction of convection of wing tip vortices and induced drag. The optimal confinement parameter and its dependence on the flight Mach number and the angle of attack was evaluated by its application to some vortex dominant flows [19]. Nevertheless, the use of the vorticity confinement method still depends on the user to adjust the confinement parameter.

Despite investigations on the topic of vorticity confinement, the way that vortices are detected in this method remains as a fundamental problem. Usually, only the existence of vorticity is the criterion for the detection of vortices; in many cases, it is not the necessary and sufficient condition. Therefore the vorticity confinement may be applied in places outside of the vortex, and thus the errors grow. Furthermore, the calculation of confinement term in these areas is waste of time. To overcome this problem, better criterions for detection of vortices must be introduced in vorticity confinement method. Different methods have been developed due to various features of a vortex.

For detecting the presence of vortex, the value of vorticity can be used as a criterion, but it can lead to some problems, in situations like boundary layer flow, etc. [20]. Lugt described that a vortex is a set of material particles rotating around a common center [21]. Hunt et al. proposed a method, known as the Q-criterion [22]. Levy et al. proposed the concept of helicity to detect vortex center [23]. Chong et al. (1990) used the eigenvalues of velocity gradient matrix [24]. Banks and Singer developed a method based on the prediction-correction mechanism to identify the vortex centers with high sensitivity [25]. Another method is based on the critical point theory, introduced by Sujudi and Haimes [26]. Moreover, Jeong and Hussein developed their method which is based on the detection of areas with minimum pressure (λ_2 method) [27]. Strawn et al. used the local maximum vorticity for the detection of vortex core [28]. Horiuti and Takagi introduced S—Ω correlation which is based on the detection of vortex sheets structure rather than vortex tube [29]. Kamkar et. al. proposed the non-dimensional form of Q, λ_2, Δ and S—Ω correlation methods [20]. Mohseni and Malek Jafarian used the vortex feature Detection

methods to improve the performance of the CVC method [1]. They define four new methods by combining four vortex feature detection methods (Q, λ_2, Δ and $S\text{–}\Omega$ correlation) with the vorticity confinement method ($FD-CVC$). In that paper, a single stationary vortex was used as a case study and more complex problems were left untouched. In the current study, the application, ability, and reliability of FD-CVC methods in more complex problems are investigated.

2 Governing Equations

Typically, vorticity confinement is applied as a source term in the governing equations. Thus in the case of 2D Euler, we have:

$$\frac{\partial \vec{W}}{\partial t}+\frac{\partial \vec{F}}{\partial x}+\frac{\partial \vec{G}}{\partial y}=\vec{S} \tag{1}$$

Where $\vec{W}$ is the flow quantities vector and $\vec{F}$ and $\vec{G}$ are flux vectors in x and y directions, respectively.

$$\vec{W}=\begin{bmatrix}\rho\\ \rho u\\ \rho v\\ \rho e_0\end{bmatrix} \tag{2}$$

$$\vec{F}=\begin{bmatrix}\rho u\\ \rho u^2+p\\ \rho vu\\ \rho uh_0\end{bmatrix} \tag{3}$$

$$\vec{G}=\begin{bmatrix}\rho v\\ \rho vu\\ \rho v^2+p\\ \rho vh_0\end{bmatrix} \tag{4}$$

h_0 and p are calculated as Eqs. (5) and (6).

$$h_0=e_0+\frac{p}{\rho} \tag{5}$$

$$p=(\gamma-1)\times\rho\times\left\{e_0-\frac{u^2+v^2}{2}\right\} \tag{6}$$

Finally, $\vec{S}$ shows the compressible vorticity confinement term (Eq. (7)).

$$\vec{S}=\begin{bmatrix}0\\ \rho\vec{f}_b\cdot\hat{\imath}\\ \rho\vec{f}_b\cdot\hat{\jmath}\\ \rho\vec{f}_b\cdot\vec{V}\end{bmatrix} \tag{7}$$

The addition of Eq. (7) to the Euler equation, transfers the vorticity back towards the vortex center as it diffuses away, (Fig. (1)).

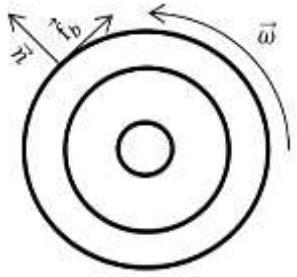

Fig 1 vorticity confinement method

Where $\vec{f}_b$ is calculated as follow:

$$\vec{f}_b = -E_c \hat{n}_c \times \vec{\omega}_z \tag{8}$$

$$\vec{\omega}_z = \frac{\partial v}{\partial x} - \frac{\partial u}{\partial y} \tag{9}$$

$$\varphi = -|\vec{\omega}_z| = -\sqrt{\omega_z^2} \tag{10}$$

The unit vector perpendicular to the vortex line ($\hat{n}_c$) is calculated as Eq. (11).

$$\hat{n}_c = \frac{\vec{\nabla}\varphi}{|\vec{\nabla}\varphi|} = \varphi_{xs}\hat{\imath} + \varphi_{ys}\hat{\jmath} \tag{11}$$

The values of φ_{ys} and φ_{xs} are calculated according to Eqs. (12) and (13).

$$\varphi_{ys} = \frac{-\varphi_y}{\sqrt{{\varphi_x}^2 + {\varphi_y}^2}} \tag{12}$$

$$\varphi_{xs} = \frac{-\varphi_x}{\sqrt{{\varphi_x}^2 + {\varphi_y}^2}} \tag{13}$$

Now Eq. (8) can be rewritten in x and y directions as follow.

$$f_{bx} = -E_c\left(|\vec{\omega}_z|\varphi_{ys}\right) \tag{14}$$

$$f_{by} = -E_c(|\vec{\omega}_z|\varphi_{xs}) \tag{15}$$

Where the parameter, E_c is known as the confinement parameter. This parameter uses to control the value of the vorticity confinement term. Now Eq. (7) is rewritten as:

$$\vec{S} = \begin{bmatrix} 0 \\ \rho f_{bx} \\ \rho f_{by} \\ \rho\left(u f_{bx} + v f_{by}\right) \end{bmatrix} \tag{16}$$

Substitution Eqs. (14) and (15) in (16) results:

$$\vec{S} = \begin{bmatrix} 0 \\ -\rho E_c|\vec{\omega}_z|\varphi_{ys} \\ \rho E_c|\vec{\omega}_z|\varphi_{xs} \\ -\rho E_c|\vec{\omega}_z|\left(u\varphi_{ys} - v\varphi_{xs}\right) \end{bmatrix} \tag{17}$$

Despite many advantages of vorticity confinement method, major problem remains. The adjustment of the confinement Parameter is still controversial. A low value of this parameter makes the vorticity confinement ineffective. On the other hand, a large value leads to oscillation and unrealistic results. Furthermore, in conventional methods, the vorticity confinement term is applied to all the domain. Thus non vortex areas like boundary layer and shear layer are affected by vorticity confinement. This can lead to errors and increasing the computational time. To solve this problem, first, the feature detection method detects the vortices, and then the CVC method is used only at these points. This idea has already been presented by the authors[1]. All of the feature detection methods are somehow use velocity gradient matrix. For example, for a 2D-flow we have:

$$\nabla\vec{V} = \begin{bmatrix} \frac{\partial u}{\partial x} & \frac{\partial u}{\partial y} \\ \frac{\partial v}{\partial x} & \frac{\partial v}{\partial y} \end{bmatrix} \tag{18}$$

This matrix can write as:

$$\nabla\vec{V} = S + \Omega \tag{19}$$

Where S and Ω are calculated as:

$$S = \frac{\nabla\vec{V} + \left(\nabla\vec{V}\right)^T}{2} \tag{20}$$

$$\Omega = \frac{\nabla\vec{V} - \left(\nabla\vec{V}\right)^T}{2} \tag{21}$$

In Eqs. (20) and (21), the superscript T means matrix transpose.
Finally, the square norm of these matrices are calculated as:

$$\|S\|^2 = \left(\frac{\partial u}{\partial x}\right)^2 + \left(\frac{\partial v}{\partial y}\right)^2 + \frac{1}{2}\left(\frac{\partial u}{\partial y} + \frac{\partial v}{\partial x}\right)^2 \tag{22}$$

$$\|\Omega\|^2 = \frac{1}{2}|\vec{\omega}_z|^2 \tag{23}$$

Four feature detection methods are introduced in the following sections.

2.1 Non-Dimensional Q Method (FDQ-CVC)

The Non-dimensional Q method is based on the Q-Criterion method [22].
Kamkar et al. proposed a Non-dimensional form of this parameter (Q) and called it the threshold function [20].

$$f_{threshold} = \frac{1}{2}\left(\frac{\|\Omega\|^2}{\|S\|^2} - 1\right) \tag{24}$$

Since the term $\|\Omega\|^2$ denotes vorticity, its zero value will indicate lack of vorticity. Therefore the threshold function tends to -0.5 in the areas outside the vortex:

$$f_{threshold} \to -\frac{1}{2} \tag{25}$$

But $\|\Omega\|^2$ will be larger than $\|S\|^2$ value inside the vortex. Thus the value of the threshold function tends to infinity:

$$f_{threshold} \to \infty \tag{26}$$

The value of the threshold function tends to -0.5, in regions, like the boundary layer and the shear layer flows. Since the strain ($\|S\|^2$) is larger than vorticity ($\|\Omega\|^2$). Therefore, these regions will not be identified as a vortex.

2.2 Non-Dimensional $\boldsymbol{\lambda_2}$ Method (FDL2-CVC)

A low pressure region can indicate the vortex center. This point was used by Jeong and Hussein as a criterion for the detection of a vortex [27]. They proposed an eigenvector-eigenvalue problem as:

$$\left[S^2 + \Omega^2 - \lambda_i I\right]X_i = 0 \tag{27}$$

They show that the negative eigenvalues indicate the existence of a low-pressure region on the plane specified with the corresponding eigenvector. Therefore, two negative eigenvalues will show vortex center. In other words, if three eigenvalues (three-dimensional problem) are considered as $\lambda_1 \le \lambda_2 \le \lambda_3$ then $\lambda_2 < 0$ indicates the presence of a vortex.

Similar to the Q criterion method Kamkar et al. Introduced a non-dimensional form of this method [20]:

$$f_{threshold} = -\frac{\lambda_2}{\|S\|^2} \tag{28}$$

2.3 Non-Dimensional Modified Δ Method (FDD-CVC)

Chong et al. introduced a method similar to the λ_2 method, They used a third-order (In 3D case) equation (Eq. (29)), [24].

$$\lambda^3 + P\lambda^2 + Q\lambda + R = 0 \tag{29}$$

The values of P, Q, and R in Eq. (29) are calculated as follows:

$$P = -trace\left[\nabla\vec{V}\right] \tag{30}$$

$$Q = \frac{1}{2}\left(P^2 - trace\left[\left(\nabla\vec{V}\right)^2\right]\right) \tag{31}$$

$$R = -det[\nabla\vec{V}] \tag{32}$$

Δ is defined as:

$$\Delta = 4RP^3 - P^2Q^2 + 4Q^3 - 18PQR + 27R^2 \tag{33}$$

In situation that $\Delta > 0$ then, The roots of Eq. (29) are as λ_r, $\lambda_{cr} \pm i\lambda_{ci}$. Where the magnitude of λ_{ci} shows the rotational strength. Therefore, it is used as the threshold function [20].

$$f_{threshold} = \frac{\lambda_{ci}}{\|S\|} \tag{34}$$

2.4 $\boldsymbol{S} - \Omega$ Correlation Method (FDSO-CVC)

In this method, an eigenvalue problem is defined similar to Δ and λ_2 methods. Horiuti et al. proposed an eigenvalue problem[28].

$$[S\Omega + \Omega S - \lambda_i I]X_i = 0 \tag{35}$$

The second answer, in terms of magnitude, is known as λ+ and represents the rotational strength. Therefore the threshold function is defined as Eq. (36) [20].

$$f_{threshold} = \frac{\lambda_+}{\|S\|^2} - 1 \tag{36}$$

The positive values of this function represent the vortex region.

3 Numerical solution Method

Integration of Eq. (1) over an elemental volume, using a finite volume method and a central difference scheme, results in Eq. (37).

$$\vec{W}^{n+1} = \vec{W}^n + RHS \tag{37}$$

Where RHS term is calculated according to Eq. (38).

$$RHS = \frac{\Delta t}{\Delta x \times \Delta y}\left(\vec{F}_{i+\frac{1}{2}} - \vec{F}_{i-\frac{1}{2}} + \vec{G}_{j+\frac{1}{2}} - \vec{G}_{j-\frac{1}{2}} - AD\right) \tag{38}$$

Where AD, represents the artificial viscosity fluxes added to the solution to eliminate oscillations and increase the stability. The fourth-order explicit Runge-Kutta method, Eqs. (39-42), is used to solve the Eq. (37), [30].

$$\overrightarrow{\mathrm{W}}^{0} = \overrightarrow{\mathrm{W}}^{\mathrm{n}} - \alpha_1 \mathrm{RHS}\left(\overrightarrow{W}^{n}\right) \quad (39)$$

$$\overrightarrow{\mathrm{W}}^{1} = \overrightarrow{\mathrm{W}}^{\mathrm{n}} - \alpha_2 RHS\left(\overrightarrow{\mathrm{W}}^{0}\right) \quad (40)$$

$$\overrightarrow{\mathrm{W}}^{2} = \overrightarrow{\mathrm{W}}^{\mathrm{n}} - \alpha_3 RHS\left(\overrightarrow{\mathrm{W}}^{1}\right) \quad (41)$$

$$\overrightarrow{\mathrm{W}}^{\mathrm{n+1}} = \overrightarrow{\mathrm{W}}^{\mathrm{n}} - \alpha_4 RHS\left(\overrightarrow{\mathrm{W}}^{2}\right) \quad (42)$$

$\overrightarrow{\mathrm{W}}^{0}$, $\overrightarrow{\mathrm{W}}^{1}$, and $\overrightarrow{\mathrm{W}}^{2}$ are the values of $\overrightarrow{\mathrm{W}}$ at each stages of the Runge-Kutta scheme. Coefficients for the corresponding 4-stage scheme are $\alpha_1 = \frac{1}{4}$, $\alpha_2 = \frac{1}{3}$, $\alpha_3 = \frac{1}{2}$, and $\alpha_4 = 1$.

Convergence testing is done by calculating the *RMS* value of the change of density and dividing it with the total number of points used in the flow domain. If this quantity is less than a user-specified value, convergence is declared.

4 Problem Definition

Two problems are considered here to demonstrate the capability of FD-CVC methods. The first problem is an axial flow around a projectile (axisymmetric). The projectile (Fig. (2)) consists of three parts of secant-ogive, cylinder with boat-tail. The second problem is a 2D flow around a square cylinder. To solve these problems, two numerical grids are generated, as shown in Figs. 3 and 4. Both of these two problems have been solved by CVC and FD-CVC methods. Finally comparing the results can provide a reasonable estimation of the performance of these methods. In each case the no-slip condition and pressure extrapolation based on the "normal momentum equation" are implicated on the wall. Mach numbers are 0.94 and 0.5 for projectile and square cylinder, respectively.

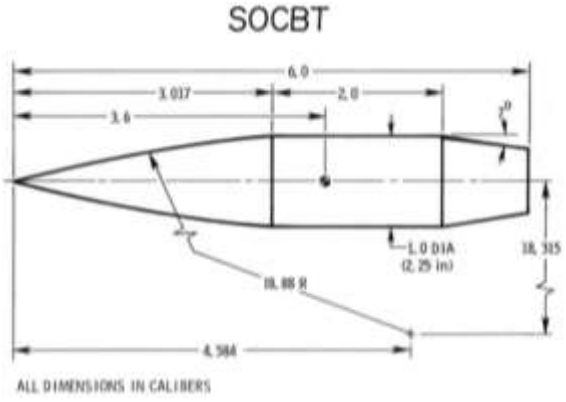

Figure 2 Schematic of the Projectile

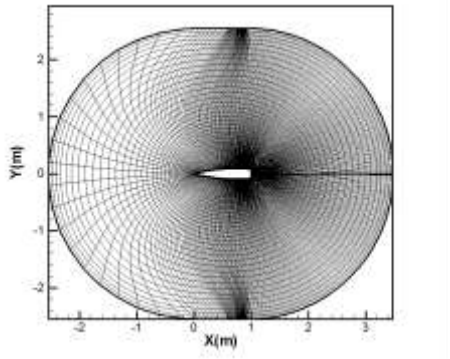

Figure 3 Solution grid around the projectile (309×50)

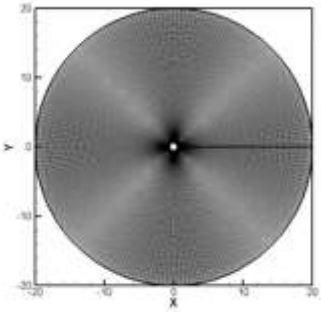

Figure 4 Solution grid for square cylinder (225×200)

5 Results

In the previous section, the problems were introduced. The results of using the FD-CVC and CVC methods are discussed as follow.

5.1 Flow over Projectile

One of the important parts to confirm results of a numerical method is checking about independence of that method from a computational grid. In this context, a mesh study has been done on the basic flow solver (described above) for flow over a projectile. Figs. 5 shows results of coefficient of pressure (C_p) around half of body with different computational grids (209*33, 255*41, 309*50 and 369*59). It should be noted that the number of meshes in two directions has increased 1.2 times. The pressure coefficient results do not show more changes for different grids, except on the cylinder part of the projectile (5>X/D>3). A strong shock wave has been formed here. It can be seen in Fig. 5 that the coarse mesh (209*33) has been able to capture the shock wave weakly. But results for other grids are considerably alike and acceptable in comparison with Kayser and Whiton experiments [31]. The results presented in these figure shows very little variation in the pressure coefficients over the range of spatial resolutions. So the 309 * 50 grid point is used for the subsequent results to obtain accurate outcomes and save the computational time.

In the case of axisymmetric flow around a projectile, the effect of using FD-CVC methods on reducing the dependence of the results on the value of confinement parameters has been investigated. The vortex status at the back of the projectile was selected as a measure of the response to the variation in the amount of confinement parameter (Figs. (6) to (15)).

Setting the value of confinement parameter equal to 0.1 results in a normal shape of wake flow (Fig.(6)). Fig. (7) shows that the wake structure becomes unphysical when the value of confinement parameter increases (E_c=0.2). On the other hand, results of using FD-CVC methods and the same values of the confinement parameters (E_c=0.1, E_c=0.2) have been shown in Figs. 8 to 15. It is observed that the unphysical vortex has been severely restricted and the dependency of the results on the value of confinement parameter has been greatly decreased. This can be seen by comparing Figs. 8 to 11 (E_c = 0.1) with Figs. 12 to 15. (E_c= 0.2).

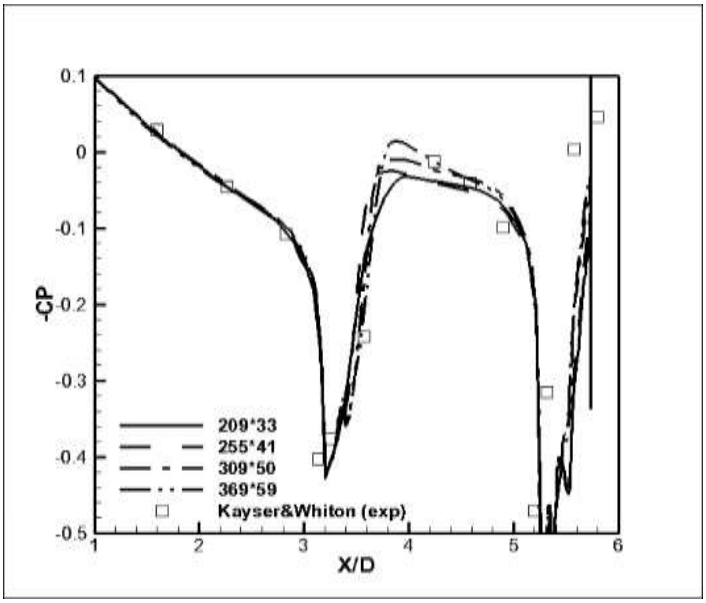

Figure 5 Coefficient of pressure as a function of X/D for various spatial resolutions

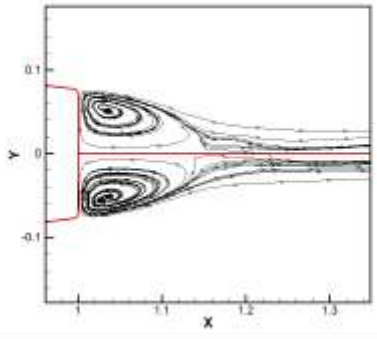

Figure 6 Streamlines behind a projectile using CVC method (E_c=0.1)

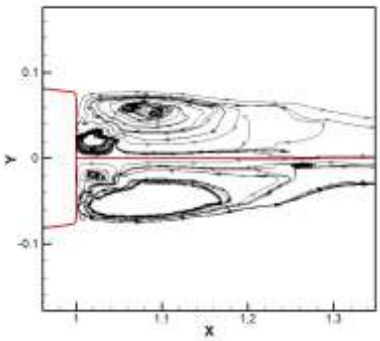

Figure 7 Streamlines behind a projectile using CVC method (E_c=0.2)

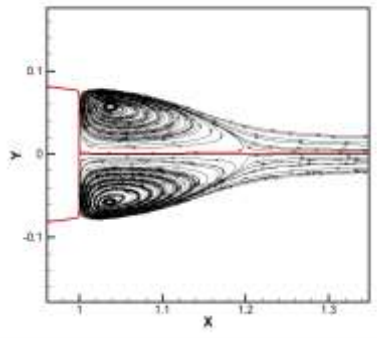

Figure 8 Streamlines behind a projectile using FDQ-CVC method (E_c=0.1)

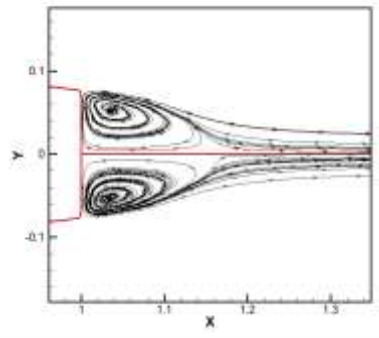

Figure 9 Streamlines behind a projectile using FDL2-CVC method (E_c=0.1)

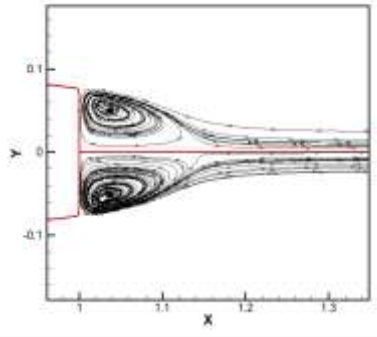

Figure 10 Streamlines behind a projectile using FDD-CVC method (E_c=0.1)

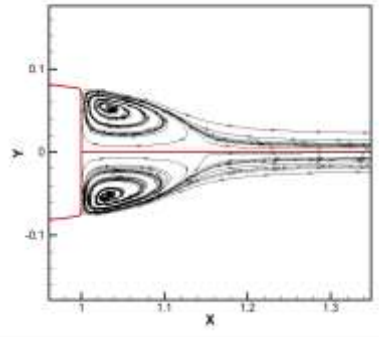

Figure 11 Streamlines behind a projectile using FDSO-CVC method (E_c=0.1)

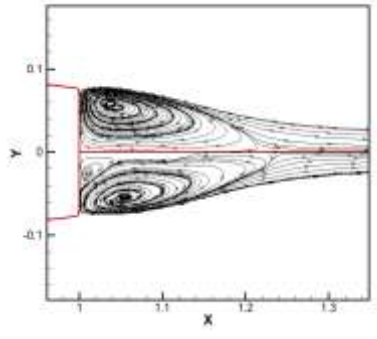

Figure 12 Streamlines behind a projectile using FDQ-CVC method (E_c=0.2)

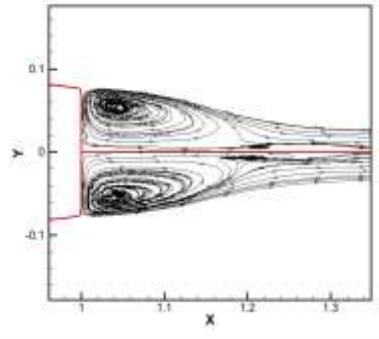

Figure 13 Streamlines behind a projectile using FDL2-CVC method (E_c=0.2)

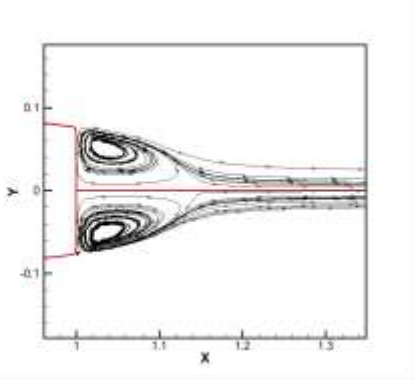

Figure 14 Streamlines behind a projectile using FDD-CVC method (E_c=0.2)

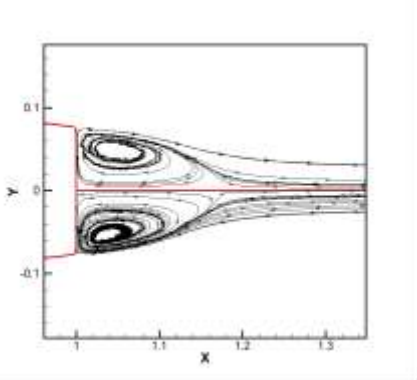

Figure 15 Streamlines behind a projectile using FDSO-CVC method (E_c=0.2)

The effect of the unphysical vortex (Fig. (7)) on pressure coefficient (C_p) distribution has been shown in Fig 16. Negative effects of the high value of confinement parameter is obvious using CVC in this figure. However, it can be seen in Figs. (17) to (20) using FD-CVC methods, C_p distribution does not disturb even by increasing the confinement parameter values. This means that the sensitivity of the results on the value of this parameter has been reduced.
The results (C_p) of FDQ-CVC and FDL2-CVC methods still show some changes as the result of increasing the value of the confinement parameter (Figs. (17) and (18)). It is also observed that the results of FDD-CVC and FDSO-CVC methods are more consistent with experimental results (Figs. (19) and (20)).

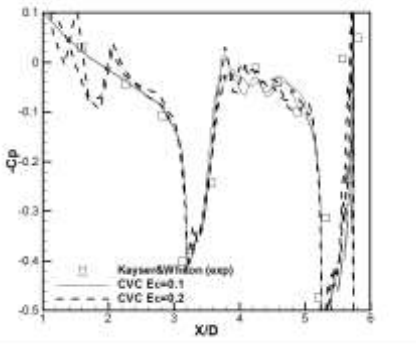

Figure 16 Effect of changes in confinement parameter on the C_p distribution using CVC method

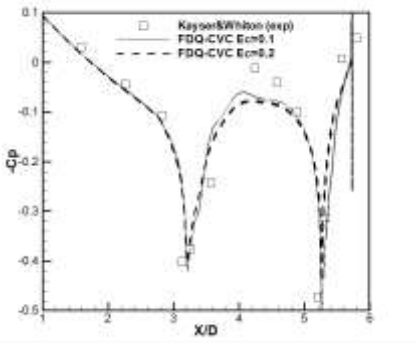

Figure 17 Effect of changes in confinement parameter on the C_p distribution using FDQ-CVC method

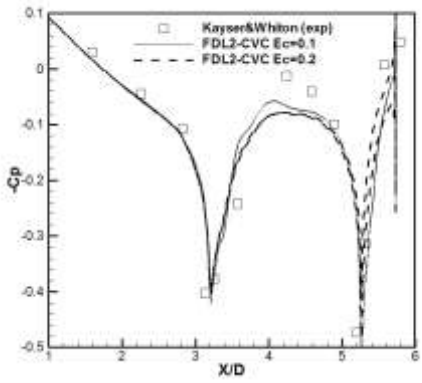

Figure 18 Effect of changes in confinement parameter on the C_p distribution using FDL2-CVC method

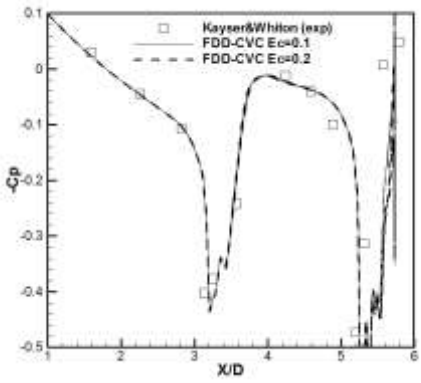

Figure 19 Effect of changes in confinement parameter on the C_p distribution using FDD-CVC method

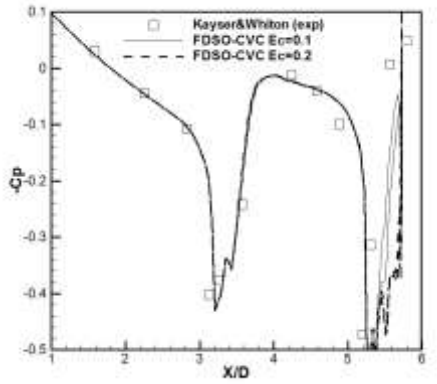

Figure 20 Effect of changes in confinement parameter on the C_p distribution using FDSO-CVC method

Despite using the same value for the confinement parameter (E_c = 0.05), the results of FDQ-CVC and FDL2-CVC methods are more consistent with the experimental data than the CVC and without CVC (W/CVC) methods (Figs. (21) and (22)).

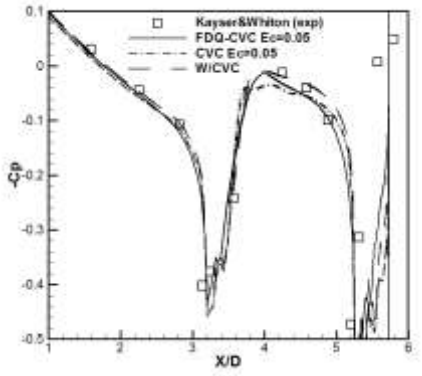

Figure 21 Comparison of the pressure coefficient distribution around the body using W/CVC, CVC, FDQ-CVC (E_c=0.05) methods and experimental results

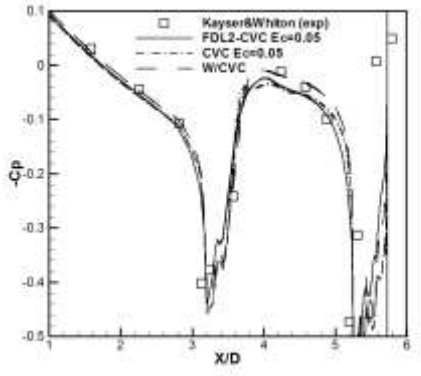

Figure 22 Comparison of the pressure coefficient distribution around the body using W/CVC, CVC, FDL2-CVC (E_c=0.05) methods and experimental results

5.2 Flow Over Square Cylinder

To investigate the reliability and advantages of FD-CVC methods, flow around a square cylinder is considered (Figs. (23) to (32)). As shown, increasing the value of confinement parameter (E_c) disturbs the pressure field, using CVC (Fig. (24)). On the other hand, the disturbances have been eliminated using FD-CVC methods (Figs. (25) to (32)).

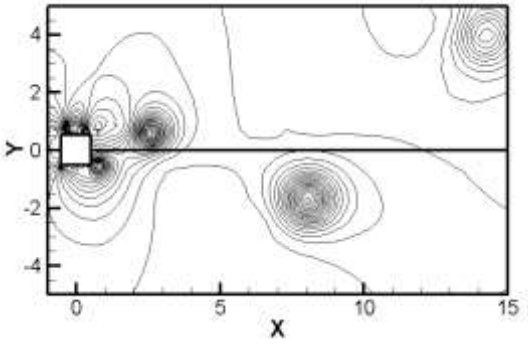

Figure 23 Pressure contours behind square cylinder using CVC method (E_c=0.1)

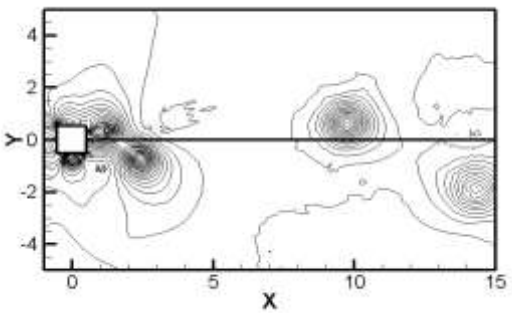

Figure 24 Pressure contours behind square cylinder using CVC method (E_c=0.2)

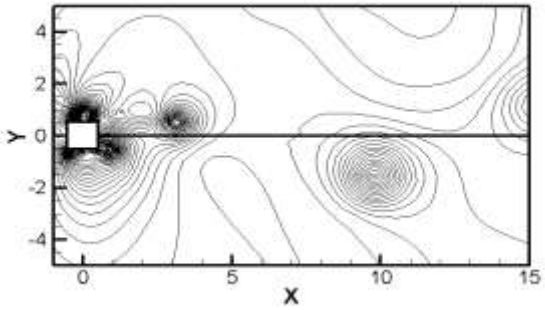

Figure 25 Pressure contours behind square cylinder using FDQ-CVC method (E_c=0.1)

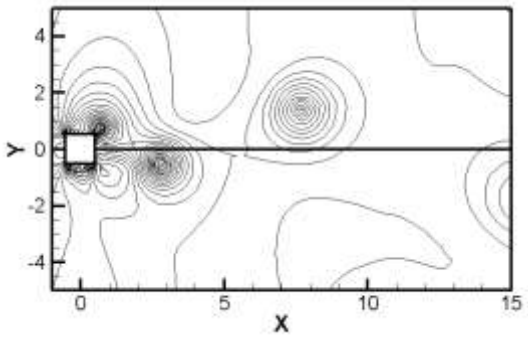

Figure 26 Pressure contours behind square cylinder using FDQ-CVC method (E_c=0.2)

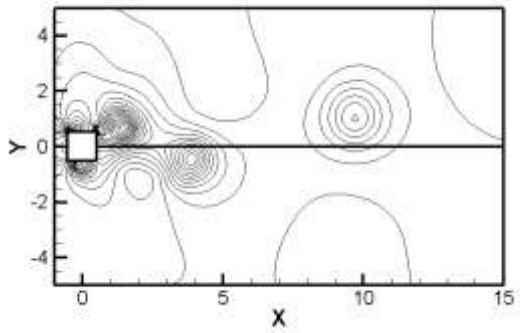

Figure 27 Pressure contours behind square cylinder using FDL2-CVC method (E_c=0.1)

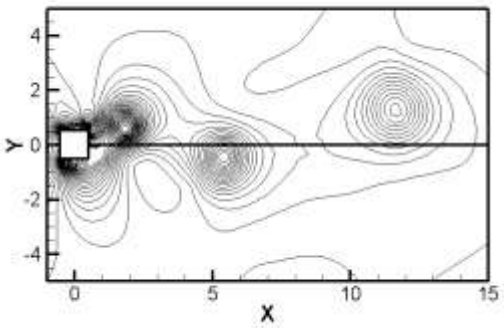

Figure 28 Pressure contours behind square cylinder using FDL2-CVC method (E_c=0.2)

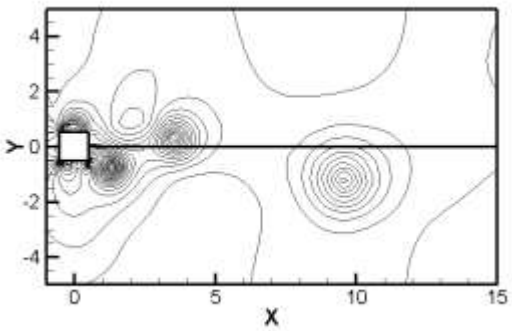

Figure 29 Pressure contours behind square cylinder using FDD-CVC method (E_c=0.1)

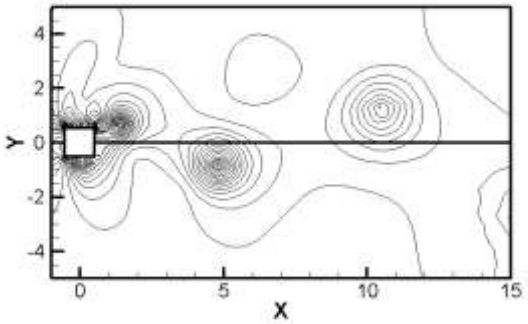

Figure 30 Pressure contours behind square cylinder using FDD-CVC method (E_c=0.2)

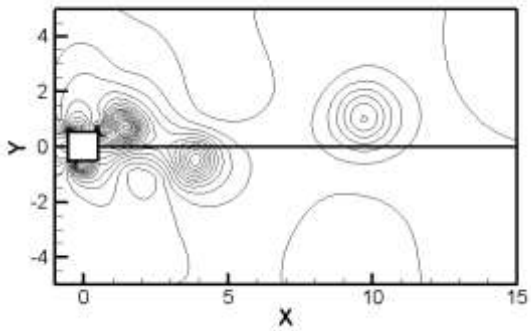

Figure 31 Pressure contours behind square cylinder using FDSO-CVC method (E_c=0.1)

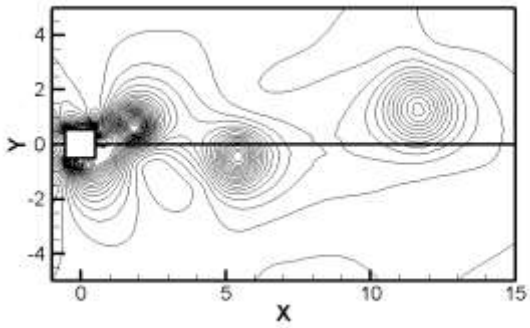

Figure 32 Pressure contours behind square cylinder using FDSO-CVC method (E_c=0.2)

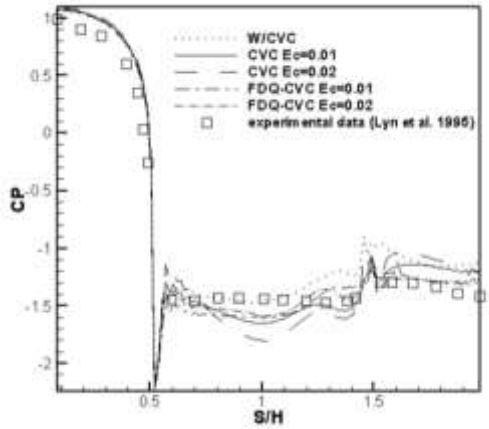

Figure 33 comparison of the pressure coefficient obtained with W/CVC, CVC, FDQ-CVC (E_c=0.01 and E_c=0.02) and experiments

6 Conclusion

The ability and flexibility of the FD-CVC methods on more complex and applied problems was investigated in this paper. An axisymmetric flow around a projectile and two-dimensional flow around a square cylinder was selected as the test cases. Results showed the preferable performance of FD-CVC methods in comparison with a simple CVC method. Briefly, it can be said:

- When using the CVC method, the results are vastly affected by changes in the value of confinement parameters to the extent that results become unphysical. But, using the FD-CVC methods this problem is solved.
- Furthermore, it can be seen that the results of FDQ-CVC and FDL2-CVC are still affected by increasing the confinement parameter value. But, FDD-CVC and FDSO-CVC methods are not suffering from this problem.
- The FDD-CVC and FDSO-CVC results are more match with experimental data.
- FD-CVC methods can reduce the sensitivity of the results on the value of confinement parameters.
- Finally, the FD-CVC methods can be used as a powerful and reliable tool for the vortex dominant flows in aerodynamics problems.

References

[1] Mohseni, M., and Malek Jafarian, S., "Improvement of Compressible Vorticity Confinement Method by Combining it with Vortex Feature Detection Methods", Journal of Applied Fluid Mechanics.,Vol. 11, pp. 1395-1406, (2018).

[2] Steinhoff, J., "*Vorticity Confinement: A New Technique for Computing Vortex Dominated Flows*", in Caughey, D., and Hafez, M. (Editors), Frontiers of Computational Fluid Dynamics, pp. 235-263, John Wiley & Sons, New York, (1994).

[3] Steinhoff, J., Mersch, T., and Decker, F., "Computation of Incompressible Flow Over Delta Wings Using Vorticity Confinement", 32th Aerospace Sciences Meeting and Exhibit, January 10-13, Reno, NV, U.S.A, pp. 646, (1994).

[4] Hu, G., Grossman, B., and Steinhoff, J., "Numerical Method for Vorticity Confinement Incompressible Flow", AIAA Journal, Vol. 40, pp. 1945-1953, (2002).

[5] Sadri, M., Hejranfar, K., and Ebrahimi, M., "On Application of High-Order Compact Finite-Difference Schemes to Compressible Vorticity Confinement Method", Aerospace Science and Technology, Vol. 46, pp. 398-411, (2015).

[6] O'Regan, M., Griffin, P., and Young, T., "A Vorticity Confinement Model Applied to URANS and LES Simulations of a Wing-Tip Vortex in the Near-Field", International Journal of Heat and Fluid Flow, Vol. 61, pp. 355-365, (2016).

[7] Costes, M., Petropoulos, I., and Cinnella, P., "Development of a Third-Order Accurate Vorticity Confinement Scheme", Computers & Fluids,Vol. 136, pp. 132-151, (2016).

[8] Petropoulos, I., Costes, M., and Cinnella, P., "Development and Analysis of High-Order Vorticity Confinement Schemes", Computers & Fluids,Vol. 156, pp. 602-620, (2017).

[9] Sidilkover, D., "Towards Unification of the Vorticity Confinement and Shock Capturing (TVD and ENO/WENO) Methods", Journal of Computational Physics, Vol. 358, pp. 235-255, (2018).

[10] Sadri, M., Hejranfar, K., and Ebrahimi, M., "Prediction of Fluid Flow and Acoustic Field of a Supersonic Jet Using Vorticity Confinement", The Journal of the Acoustical Society of America, Vol. 144, pp. 1521-1527, (2018).

[11] Wen, J., and Ma, H., "Real-Time Smoke Simulation Based on Vorticity Preserving Lattice Boltzmann Method", The Visual Computer, Vol. 35, pp.1279-1292, (2019).

[12] Costes, M., and Kowani, G., "An Automatic Anti-Diffusion Method for Vortical Flows Based on Vorticity Confinement", Aerospace Science and Technology, Vol. 7, pp. 11-21, (2003).

[13] Robinson, M., "Application of Vorticity Confinement to Inviscid Missile Force and Moment Prediction", 42th AIAA Aerospace Sciences Meeting, January 5-8, Reno, NV, U.S.A, pp. 717, (2004).

[14] Jafarian, M.M., and Fard, M.P., "Development and Application of Compressible Vorticity Confinement", Scientia Iranica, Vol. 14, pp. 251-262, (2007).

[15] Butsuntorn, N., and Jameson, A., "Time Spectral Method for Rotorcraft Flow", 46th AIAA Aerospace Sciences Meeting and Exhibit, January 7-10, Reno, NV, U.S.A, pp. 403 ,(2008).

[16] Hahn, S., and Iaccarino, G., "Towards Adaptive Vorticity Confinement", 47th AIAA Aerospace Sciences Meeting and Aerospace Exposition, January 5-8, Reno, NV, U.S.A, pp. 1613, (2009).

[17] Bagheri-Esfeh, H., and Malek-Jafarian, M., "Development of Artificial Dissipation Schemes and Compressible Vorticity Confinement Methods", Proceedings of the Institution of Mechanical Engineers, Part G: Journal of Aerospace Engineering, Vol. 225, pp. 929-945, (2011).

[18] Mohseni, M., and Malek jafarian, M., "Investigating Effect of Applying FCT Scheme in Vorticity Confinement Method on Reducing the Influence of Confinement Parameter on the Final Solution", Modares Mechanical Engineering, Vol. 18, pp. 65-74, (2018).

[19] Povitsky, A., and Pierson, K.C., "Vorticity Confinement Applied to Accurate Prediction of Convection of Wing Tip Vortices and Induced Drag", International Journal of Computational Fluid Dynamics, Vol. 35, pp. 143-156, (2021).

[20] Kamkar, S., Jameson, A., and Wissink, A.M., "Automated Grid Refinement using Feature Detection", 47th AIAA Aerosciences Conference, January 5-8, Reno, NV, U.S.A, pp. 1496, (2009).

[21] Lugt, H.J., "*The Dilemma of Defining a Vortex*", in Müller, U., Roesner, K.G., Schmidt, B. (Editors), Recent Developments in Theoretical and Experimental Fluid Mechanics, pp. 309-321, Springer Berlin, Heidelberg, (1979).

[22] Hunt, J.C., Wray, A.A., and Moin, P., " Eddies, Streams, and Convergence Zones in Turbulent Flows", Proceedings of the 1988 Summer Program, Vol. 193, pp. 193-208, (1988).

[23] Levy, Y., Degani, D., and Seginer, A., "Graphical Visualization of Vortical Flows by Means of Helicity", AIAA Journal, Vol. 28, pp. 1347-1352, (1990).

[24] Chong, M.S., Perry, A.E., and Cantwell, B.J., "A General Classification of Three-Dimensional Flow Fields", Physics of Fluids A: Fluid Dynamics, Vol. 2, pp. 765-777, (1990).

[25] Banks, D.C., and Singer, B.A., "Vortex Tubes in Turbulent Flows: Identification, Representation, Reconstruction. Visualization", Proceedings Visualization' 94, October 17-21, Washington, DC, U.S.A., pp. 132-139, (1994).

[26] Sujudi, D., and Haimes, R.," Identification of Swirling Flow in 3D Vector Fields", 12th Computational fluid dynamics conference, June 19-22, San Diego, CA, U.S.A, pp. 1715, (1995).

[27] Jeong, J., and Hussain, F., "On the Identification of a Vortex", Journal of Fluid Mechanics, Vol. 285, pp. 69-94, (1995).

[28] Strawn, R.C., Kenwright, D.N., and Ahmad, J., "Computer Visualization of Vortex Wake Systems", AIAA J., Vol. 37, pp. 511-512, (1999).

[29] Horiuti, K., and Takagi, Y., "Identification Method for Vortex Sheet Structures in Turbulent Flows", Physics of Fluids, Vol. 17, pp. 121703, (2005).

[30] Jameson, A., Schmidt, W., and Turkel, E., "Numerical Solutions of the Euler Equations by Finite Volume Methods Using Runge-Kutta Time-stepping Schemes", 14th fluid and plasma dynamics conference, June 23-25, Palo Alto, CA, U.S.A, pp.1259, (1981).

[31] Kayser, L., and Whiton, F., "Some Aerodynamic Characteristics of a Projectile Shape with a Nonaxisymmetric Boattail at Mach Numbers of 0.91 and 3.02", Army Ballistic Research Lab Aberdeen Proving Ground MD, DOI:10.21236/ada133755, (1983).

[32] Lyn, D., Einav, S., Rodi, W., and Park, J.H., "A Laser-Doppler Velocimetry Study of Ensemble-Averaged Characteristics of the Turbulent Near Wake of a Square Cylinder", Journal of Fluid Mechanics, Vol. 304, pp. 285-319, (1995).

Nomenclature

e_0	Internal Energy (J/kg)
E_c	Confinement Parameter
$\vec{F}$	Flux Vector in x Direction
$\vec{f}_b$	Body Force Vector in Source Term $(kg \cdot m/sec^2)$
f_{bx} , f_{by}	Body Force of x and y Momentum Equations $(kg \cdot m/sec^2)$
$f_{threshold}$	Threshold Function
$\vec{G}$	Flux Vector in y Direction
h_0	Total Energy (J/kg)
I	Identity Matrix
$\hat{n}$	Unit Vector Perpendicular to the Vortex line
$\hat{\imath}$, $\hat{\jmath}$	Unit Vectors
p	Pressure (Pa)
RHS	Residual
$\vec{S}$	Source Term Vector
S	Strain-rate tensor
t	Time (sec)
u,v	Velocity Magnitude in x and y Directions (m/sec)
$\vec{V}$	Velocity Vector (m/sec)
$\vec{W}$	Flow Quantitative Vector
X	Eigenvector
x,*y*	Coordinate Directions (m)
α	Coefficients of Runge-Kutta Scheme
γ	Heat Capacity Ratio
$\Delta x, \Delta y$	Mesh size in x and y directions
Δt	Time step size
λ	Eigenvalue
ρ	Density (kg/m^3)
φ	Vorticity Magnitude $(1/sec)$
$\varphi_{xs}, \varphi_{ys}$	Components of Unit Vector Perpendicular to the Vortex line
ω	Vorticity $(1/sec)$
Ω	rotational tensor